



## Original article

## Recombinant Human erythropoietin reduces viability of MCF-7 breast cancer cells from 3D culture without caspase activation

Hareth Y. ShujaaEdin<sup>a</sup>, Nagi A. AL-Haj<sup>b,\*</sup>, Abdullah Rasedee<sup>c,\*</sup>, Noorjahan Banu Alitheen<sup>d</sup>, Arifah Abdul Kadir<sup>c</sup>, Chee Wun How<sup>e</sup>, Heshu Sulaiman Rahman<sup>f</sup>, Al-Shwyeh Hussah Abdullah<sup>g</sup><sup>a</sup> Institute of Bioscience, Universiti Putra Malaysia, Malaysia<sup>b</sup> Faculty of Medicine and Health Sciences, Sana'a University, Yemen<sup>c</sup> Faculty of Veterinary Medicine, Universiti Putra Malaysia, Malaysia<sup>d</sup> Faculty of Biotechnology and Biomolecular Sciences, University Putra Malaysia, Malaysia<sup>e</sup> School of Pharmacy, Monash University Malaysia, Bandar Sunway, Selangor, Malaysia<sup>f</sup> College of Medicine, University of Sulaimani, Kurdistan Region, Iraq<sup>g</sup> College of Science, Imam Abdul Rahman bin Faisal University, Saudi Arabia

## ARTICLE INFO

## Article history:

Received 17 November 2020

Revised 18 January 2021

Accepted 28 January 2021

Available online 11 February 2021

## Keywords:

Recombinant human erythropoietin  
MCF-7 cell

2-dimensional MCF-7 cell culture

3-dimensional MCF-7 cell culture

## ABSTRACT

Recombinant human erythropoietin (rHuEPO) is the erythropoiesis-stimulating hormone that is being used concurrently with chemotherapeutic drugs in the treatment of anemia of cancer. The effect of rHuEPO on cancer cells in 3-dimensional (3D) cultures is not known. The objective of the study was to determine the effect of rHuEPO on the viability of MCF-7 breast cancer cells from 2-dimensional (2D) and 3D cell cultures. The monolayer MCF-7 cells from 2D culture and MCF-7 cell from 3D culture generated by ultra-low adhesive microplate technique, were treated with 0, 0.1, 10, 100 or 200 IU/mL rHuEPO for 24, 48 or 72 h. The effects of rHuEPO on MCF-7 cell viability and proliferation were determined using the (4,5-dimethylthiazol-2-yl)-2,5-diphenyl tetrazolium bromide assay (MTT), neutral red retention time (NRR), trypan blue exclusion assay (TBE), DNA fragmentation, acridine orange/propidium iodide staining (AO/PI) assays. The MCF-7 cells for 3D culture were also subjected to caspase assays and cell cycle analysis using flow cytometry. rHuEPO appeared to have greater effect at lowering the viability of MCF-7 cells from 3D than 2D cultures.

rHuEPO significantly ( $p < 0.05$ ) decreased viability and down-regulated the caspase activities of 3D MCF-7 cells in dose- and time-dependent manner. The cell cycle analysis showed that rHuEPO caused MCF-7 cells to enter the subG0/G1 phase. Thus, the study suggests that rHuEPO has a cytostatic effect on the MCF-7 breast cancer cells from 3D culture.

© 2021 The Author(s). Published by Elsevier B.V. on behalf of King Saud University. This is an open access article under the CC BY-NC-ND license (<http://creativecommons.org/licenses/by-nc-nd/4.0/>).

**Abbreviations:** rHuEPO, recombinant human erythropoietin; MTT, (4,5-dimethylthiazol-2-yl)-2,5-diphenyl tetrazolium bromide assay; NRR, neutral red retention; TBE, trypan blue exclusion; AO/PI, acridine orange/propidium iodide staining; ULAT, ultra-low adhesion technique; FBS, fetal bovine serum.

\* Corresponding authors.

E-mail addresses: [naji\\_ahmed@upm.edu.my](mailto:naji_ahmed@upm.edu.my) (N.A. AL-Haj), [rasedee@upm.edu.my](mailto:rasedee@upm.edu.my) (A. Rasedee).

Peer review under responsibility of King Saud University.



## 1. Introduction

Erythropoietin (EPO) receptor (EPOR) is not only expressed on erythroid progenitors but also on some cancer cells (Acs et al., 2001; Cao et al., 2010; Ilkovičová et al., 2017; Teo et al., 2020), including the breast cancer cells (Todaro et al., 2013; Reinbothe et al., 2014). The EPO pleiotropic effects extend beyond erythropoiesis, to include modification of innate immunity to infections and inflammation (Nairz et al., 2011), growth stimulation of normal or cancer cells (Fujisue et al., 2013), tissue protection (Nangaku, 2013), and anti-apoptosis (Wang et al., 2015). In cancers, EPO was shown to enhance the proliferation and survival of tumors (Fujisue et al., 2013; Tankiewicz-Kwedlo et al., 2016); however, the effect is not the same for all tumors. The effects of EPO

depend on experimental conditions, target cells and tissues. For example, in rats with partial hepatectomy, multiple doses of EPO increased hepatocellular apoptosis and inhibited liver regeneration (Klemm et al., 2008). On the other hand, EPO inhibited the proliferation of T-cells without causing cell death (Cravedi et al., 2014) while carbamylated EPO decreased proliferation and neurogenesis in the sub-ventricular zone of the rat brain (Osato et al., 2018). On cancer cells, the growth-stimulation effect of EPO is not primarily through membrane EPORs; in fact, the stimulatory effect of EPO is still evident in cells devoid of the receptor (Okazaki et al., 2008).

Currently, almost all *in vitro* cancer studies used 2D cell culture models to determine the effects of drugs and potential therapeutic compounds. This is also true for investigations on the effect of EPO as adjuvant therapy in the treatment cancer-related anemia. Although many cancer cells possess EPOR, the *in vitro* effect of EPO on these cells remains debatable (Debeljak et al., 2014). In 2D cultures, one study showed that EPO had no tumor-promoting effect on the non-small cell lung cancer cell line (Frille et al., 2018) while another showed EPO stimulated epithelial-mesenchymal transition inducing proliferation of renal cell carcinoma (Morais et al., 2013).

The 3D not the 2D cancer model mimics *in vivo* tumors (Riffle and Hedge, 2017). Thus, it is conceivable that the effects of EPO on cells from 2D and 3D cultures would differ. To the best of our knowledge, this is the first study that investigated the effect of rHuEPO on the viability of MCF-7 breast cancer cells grown in 3D cultures.

## 2. Materials and methods

### 2.1. MCF-7 2D culture

MCF-7 cells (passage number < 10) were cultured in T-75 flask containing 10 mL RPMI1640 medium (Gibco™ cell culture media, Fisher Scientific), supplemented with 10% heat-inactivated fetal bovine serum (iFBS) and 1% of penicillin/streptomycin (Gibco™, Fisher Scientific). The cells were incubated in 5% CO<sub>2</sub> incubator at 37 °C and 95% humidity with medium change every second day. Upon reaching 85% confluency, the cells were washed with cold phosphate-buffered saline (PBS) and detached with 5 mL TrypLE™ Express Enzyme (Fisher Scientific). Then TrypLE™ was neutralized with ice-cold culture medium containing 10% FBS and the cells pelleted by centrifuging at 200 × g (Eppendorf AG, Hamburg, Germany) for 5 min. The cells were re-suspended and counted, processed for the seeding of 3D MCF-7 culture to obtain MCF-7 cell spheroids. The cell suspension containing 4 × 10<sup>4</sup> and 3 × 10<sup>5</sup> cells/mL in 200 μL was seeded into a 96-well plate for determination of cell response to rHuEPO using the MTT and neutral red retention time (NRRT) assays, respectively. Cell suspensions containing 1.25 × 10<sup>5</sup> cells/mL were seeded into a 6-well plate for the determination of cell response to rHuEPO using TBE, caspase activity, DNA fragmentation, and AO/PI staining assays and cell cycle analysis.

### 2.2. MCF-7 3D culture

The MCF-7 cell spheroid from 3D culture used in the study were generated using the ultra-low adhesion technique (ULAT) technique. 300 μL cell suspension containing 1.6 × 10<sup>4</sup> cells/mL were dispensed in each well of a 96-well conical-bottomed microplate (Nunc® MicroWell™ 96-well polystyrene plates, USA). The cells were cultured in RPMI1640 medium (Gibco™ cell culture media, Fisher Scientific), supplemented with 10% heat-inactivated fetal bovine serum (iFBS) and 1% of penicillin/streptomycin (Gibco™, Fisher Scientific, USA), and incubated in the 5% CO<sub>2</sub> incubator at

37 °C and under 95% humidity. After treatment with rHuEPO, single cells obtained from the disruption of MCF-7 cell spheroids were manipulated similarly to monolayer cells from 2D cultures. The cells were then subjected to the determination of cell response to rHuEPO treatment via cell viability assays; MTT, NRRT, TB, DNA fragmentation, and AO/PI staining caspases and cell cycle analysis.

### 2.3. rHuEPO treatment

Stock solution was prepared by dissolving rHuEPO (EPREX 10,000 IU/mL, Janssen-Cilag Ltd, Switzerland) in RPMI1640 medium without fetal bovine serum (FBS). Before treatment, the cells from the 2D and 3D cultures were deprived of FBS for 18 h before treatment. Then, the 2D and 3D culture cells were maintained in RPMI1640 medium supplemented with 2% FBS during treatment. After washing with PBS, single cell suspensions were obtained by dissociating the attached cells using TrypLE™ Express Enzyme (Thermo Fisher Scientific, USA) according to manufacturer's instruction. TrypLE was then neutralized with medium containing 10% FBS. 3D cell spheroids, before disruption, were similarly treated with rHuEPO at concentrations equal to those used for the 2D culture.

### 2.4. MTT assay

#### 2D culture

Single cell suspensions from 2D MCF-7 cell culture in 200 μL medium containing 4 × 10<sup>4</sup> cells/mL were seeded into each well of a 96-well microplate. Then the cells were treated with 0, 1.56, 3.13, 6.25, 12.5, 25, 50, 100 or 200 IU/mL rHuEPO for 24, 48 or 72 h for determination of cell viability. Untreated cells were used as the control.

#### 3D culture

Each well of a 96-well microplate was seeded with 8 to 10 small MCF-7 cell spheroids and the spheroids treated with various concentrations of rHuEPO, as described for the 2D cells. The spheroids were incubated with PBS then mixed with TrypLE™ Express Enzyme (Thermo Fisher Scientific, USA) with multiple pipetting to dissociate the cells and obtain single cell suspensions. 200 μL of 5 × 10<sup>5</sup> cells/mL of single cell suspensions were seeded to each well of 96-microwell plate for MTT assay. The plates were centrifuged at 200 × g (Eppendorf AG, Hamburg, Germany) for 5 min to allow the cells to settle down at the bottom of the well. The plates were incubated for 3 h to allow for cells attachment.

The MTT assay was conducted according to the method described by (Mosmann 1983, Kumar et al., 2018) Briefly, the RPMI1640 medium in the single cell suspensions from 2D and 3D cell cultures were discarded and cells washed gently with PBS. 20 μL of MTT dye in RPMI1640 medium were added to each well and the plate incubated in dark for 4 h. The RPMI1640 medium was carefully discarded without disrupting the cell colonies and 100 μL DMSO was added to each well to dissolve the formazan crystals. The plate was incubated for 30 min and read in the ELISA reader (ELx800 Absorbance Microplate Reader, BioTek, US) at 570 nm. The cell viability was calculated using the following formula:

$$\text{Cell viability (\% of Control)} = \frac{\text{OD of treated cells}}{\text{OD of control cells}}$$

where the OD is the optical density that is proportional to the concentration of viable cells.

### 2.5. Neutral red retention time (NRRT) assay

200 μL of 5 × 10<sup>3</sup> cells/mL of MCF-7 cell suspensions from 2D and pretreated 3D cultures treated with 0, 0.1, 10, 100 or 200 IU/mL rHuEPO for 24, 48, or 72 h were seeded in a 96-well microplate.

The same quantity of untreated cells served as the control. Then 200  $\mu\text{L}$  medium containing of 45  $\mu\text{g}/\text{mL}$  neutral red was added to each well and the plate incubated for 3 h at room temperature. The plates were centrifuged for  $200 \times g$  (Eppendorf AG, Hamburg, Germany) for 5 min to allow the cells to settle at the bottom of the well before incubating for 3 h with 45  $\mu\text{g}/\text{mL}$  neutral red dye at room temperature. After discarding the supernatant, 150  $\mu\text{L}$  of fixing solution (1%  $\text{CaCl}_2$ , 0.5% formaldehyde in milliQ water) was added to each well and the cells allowed to stand for 2 min before washing twice with PBS. 100  $\mu\text{L}$  dissolving solution (1% acetic acid, 50% ethanol in milliQ water) were added to each well and the plate incubated at room temperature for 10 min. The absorbance was determined at 540 nm in the ELISA reader (ELx800 Absorbance Microplate Reader, US). The cell viability was calculated and expressed as percentage of the control, as described in the section 2.4.

### 2.6. Trypan blue exclusion (TBE) assay

200  $\mu\text{L}$  of  $5 \times 10^3$  cells/mL MCF-7 cell suspensions from 2D and 3D cultures that were treated with 0, 0.1, 10, 100 or 200 IU rHuEPO for 24, 48 and 72 h and seeded in a 96-microwell plate were subjected to the TBE assay (Louis and Siegel, 2011). Trypan blue solution (0.4%) (Sigma-Aldrich) was mixed with the cell suspensions at a ratio of 1:1 and 20  $\mu\text{L}$  was placed on hemocytometer. Dark blue-stained cells and TBE cells were counted and cell viability determined using the following formula:

$$\text{Cell viability (\%)} = \frac{\text{Number of unstained treated cells}}{\text{Number of unstained non - treated cells}} \times 100$$

### 2.7. DNA fragmentation assay

$2.5 \times 10^6$  single cell MCF-7 cell suspensions from 2D and 3D cultures that were treated with 0, 10, or 200 IU/mL rHuEPO for 72 h were subjected to DNA fragmentation assay. Diphenylamine (DPA) stain was used in the quantification of fragmented DNA (Suenobu et al., 1999; Burton, 1956). The cells were harvested and lysed with 0.4 mL of cellular lysis solution (10 mmol/L Tris, 1 mmol/L EDTA, and 0.1% NP-40, pH 7.5). Cell lysates were centrifuged at  $13,000 \times g$  for 10 min to sediment intact chromosomal DNA and leaving fragmented DNA in the supernatant. The supernatant were carefully collected in fresh microfuge tubes. Both tubes containing sediment and supernatant were incubated in 12.5% trichloroacetic acid (TCA) overnight at 4°C to precipitate. The following day, the sediments were centrifuged at  $13,000 \times g$  for 4 min. The DNA precipitate was hydrolyzed in 160  $\mu\text{L}$  5% Trichloroacetic acid (TCA) at 90 °C for 10 min. 320  $\mu\text{L}$  DPA solution (15 mg DPA, 150  $\mu\text{L}$   $\text{H}_2\text{SO}_4$ , and 50  $\mu\text{L}$  acetaldehyde per 10 mL glacial acetic acid) was added to each tube. 200  $\mu\text{L}$  aliquots of the solution were obtained and the absorbance read spectrophotometrically at 600 nm, using 5% TCA as the blank. The ratio of supernatant absorbance to the sum of supernatant and sediment absorbance was expressed as percentage relatively to fragmented DNA.

### 2.8. Acridine orange and propidium iodide double staining

200  $\mu\text{L}$  of  $3 \times 10^6$  cells/mL of MCF-7 single cell suspensions from 2D and 3D cell cultures that were treated with 0, 10 or 200 IU/mL rHuEPO for a period of 72 h were subjected to acridine orange (AO)/PI double staining assay (Bank, 1988). Briefly, the cells were washed with cold PBS and pelleted down by centrifugation at  $200 \times g$  (Eppendorf AG, Hamburg, Germany) for 5 min and resuspended to obtain  $1 \times 10^6$  cell/mL suspensions. Then, 10  $\mu\text{L}$  of the cell suspension were mixed with fresh 10  $\mu\text{L}$  AO/PI stain solution

(50  $\mu\text{g}/\text{mL}$ ) and the cells immediately examined under fluorescence confocal microscopy (FV1000 viewer Olympus, Japan).

### 2.9. Cell cycle assay

$2.5 \times 10^6$  single cell MCF-7 cell suspensions from 3D cell cultures that were treated with 0, 0.1, 10, 100 or 200 IU/mL EPO for 24, 48 or 72 h were subjected to cell cycle analysis (Pożarowski and Darzynkiewicz, 2004). The cells were washed with PBS containing 0.1% sodium azide and fixed with 500  $\mu\text{L}$  80% cold ethanol, dropwise with vortexing to prevent aggregation and incubated with propidium iodide (PI) for 30 min in dark. RNase enzyme was used to ensure that there was no RNA interference during the assay. The cells were examined for their DNA content in the FACS Calibur flow cytometer by laser emitting excitation light at 488 nm (Becton Dickinson, USA) and the graph of gating were generated to determine the percentage of cells at the various cell cycle phases (CellQuest software, Becton Dickinson, USA).

### 2.10. Caspase -3, -8, and -9 activities

The caspase activities were determined on MCF-7 cells from the 3D culture. 200  $\mu\text{L}$  of  $3 \times 10^6$  cells/mL MCF-7 cell suspensions that were treated with 0, 1, 10 or 200 IU/mL rHuEPO for 72 h were subjected to caspase assays using the Caspase Colorimetric Assay kits (Genscript Corporation Inc, Piscataway, NJ, USA). The extinction values were determined spectrophotometrically in a microplate reader (ELx800 Absorbance Microplate Reader, US) at 405 nm. Caspases concentrations were expressed as absorbance percentage of the control.

### 2.11. Statistical analysis

All experiments were performed in triplicates. Values were expressed as percentage of controls. When the groups met the statistical assumptions; ANOVA test was used to determine significance difference. Data that did not meet the statistical assumptions; nonparametric test, Mann-whitney U were used.  $p < 0.05$  was considered significance. These statistical procedures were performed using SPSS software program.

## 3. Results

### 3.1. Comparison of rHuEPO effect between MCF-7 cells from 2D and 3D cultures

#### 3.1.1. MTT assay

There was no significant ( $p > 0.05$ ) difference in viability among cells of different treatment groups of 2D culture. The results suggest that rHuEPO did not affect viability of MCF-7 cells from the 2D culture (Fig. 1 (A)). In contrast, rHuEPO treatments beginning at 50 IU/mL, dose- and time-dependently decreased ( $p < 0.05$ ) viability of MCF-7 cells of the 3D cell culture (Fig. 1 (B)). The greatest effect was with 200 IU/mL rHuEPO treatment for 72 h with MCF-7 cell viability decreasing to 70.22% of the control cells.

#### 3.1.2. Neutral red retention time assay

The NRRT assay showed that rHuEPO did not significantly ( $p > 0.05$ ) affect viability of 2D MCF-7 cells, irrespective of time or dose of exposure (Fig. 1(C)). In contrast, rHuEPO, in time- and dose-dependent manner, significantly ( $p < 0.05$ ) reduced the viability of MCF-7 cells from the 3D cell cultures (Fig. 1 (D)). The most significant reduction in MCF-7 cell viability was with 200 IU/mL rHuEPO after 72 h of treatment, at 69.23% viability, in comparison with the non-treated control.

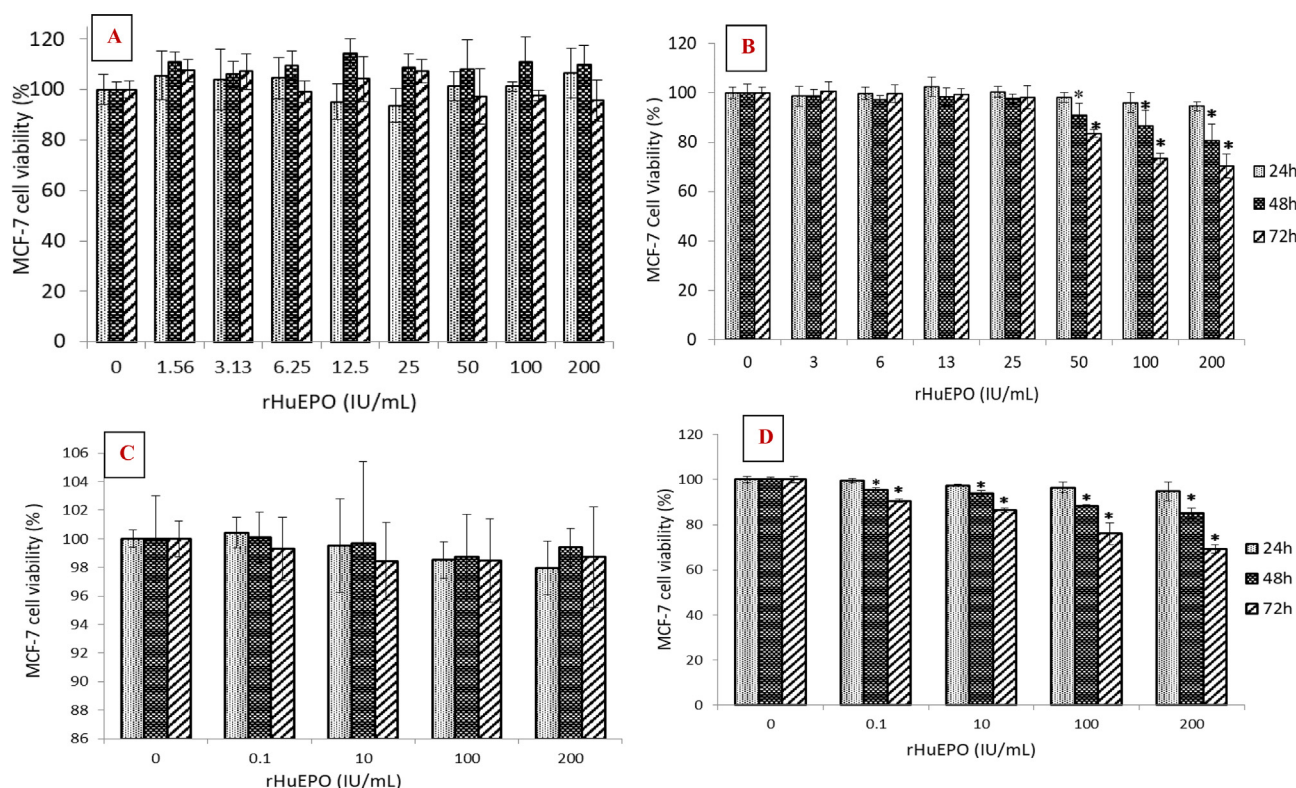


**Fig. 1.** (A) Effect of rHuEPO on viability of MCF-7 cells from 2D cultures determined by MTT assay. There is no significant difference among cells treated with various concentrations of rHuEPO. (B) Effect of rHuEPO on viability of MCF-7 cells from 3D cell cultures determined by MTT assay. rHuEPO at high concentrations, time- and dose-dependent decreased cell viability. (C) Effect of rHuEPO on viability of MCF-7 cells from 2D cultures determined by neutral red retention time assay. MCF-7 cell viability not significantly ( $p > 0.05$ ) affected by rHuEPO treatment. (D) Effect of rHuEPO on viability of MCF-7 cells from the 3D cultures determine by neutral red retention assay. MCF-7 cell viability decreased significantly ( $p > 0.05$ ) with rHuEPO treatment, even the lowest concentration of 0.1 IU/mL. Viability is expressed as % of control. \*For each treatment period, means significantly different ( $p < 0.05$ ) from control means. Error bars represent RSE.

### 3.1.3. Trypan blue exclusion assay

The TBE assay was also employed to determine the viability of MCF-7 cells. rHuEPO did not show any difference ( $p > 0.05$ ) in effect on the viability between cells from the 2D and 3D MCF-7 cultures (Fig. 2 (A) and (B)). However, rHuEPO especially at high concentrations and after 48 and 72 h of exposure appeared to be more effective at reducing viability of MCF-7 cells from 3D and 2D cultures.

### 3.1.4. DNA fragmentation

DNA fragmentation assay is a method to determine apoptosis in treated MCF-7 cells. In this study, there was no significant difference ( $p > 0.05$ ) in DNA fragmentation between rHuEPO-treated and untreated MCF-7 cells (Fig. 2 (C)). The results showed that rHuEPO treatment did not cause MCF-7 cell apoptosis, irrespective whether the cells were from 2D or 3D culture.

### 3.1.5. Acridine orange/propidium iodide staining

With the exception of a few necrotic cells, the MCF-7 cells from the 2D and 3D cultures treated with rHuEPO showed normal morphology. There is no significant difference ( $p > 0.05$ ) in morphology or degree of necrosis between the rHuEPO-treated 3D culture cells and non-treated control cells (Fig. 3).

## 3.2. Effect of rHuEPO on MCF-7 from 3D cell culture

### 3.2.1. Cell cycle

#### Treatment concentration

The most significant effect of rHuEPO on the cycle of MCF-7 cells from 3D culture was on the SubG0/G1 and G + M2 phases. The effect was concentration-dependent. rHuEPO especially at the high concentration of 200 IU/mL, markedly increased number

of MCF-7 cells entering the quiescent SubG0/G1 phase while decreasing number of cells in the G2 + M phase. After 24 h of treatment, the number of cells in the SubG0/G1 phase was > 600% higher while those in the G2 + M phase was approximately 100% lower than in the control (Fig. 4 (A)). After 48 and 72 h, the number of cells in the SubG0/G1 phase decreased to approximately 140 (Fig. 4 (B)) and 250% of control values (Fig. 4 (C)), respectively. The number of cells in the S and G0/G1 phases essentially remained similar to that of the control irrespective of rHuEPO treatment concentrations and exposure time. The result showed that rHuEPO especially at high concentrations increased and decreased the population of MCF-7 cells in the SubG0/G1 and G + M2, respectively.

#### Time of exposure

rHuEPO treatment period produced a peculiar effect on the cycles of 3D culture MCF-7 cells. The populations of MCF-7 cells treated with rHuEPO at all concentrations were high in the SubG0/G1 phase, decreased markedly at 48 and increasing again to high numbers at 72 h of treatment (Fig. 5 (A-D)). The effect of rHuEPO on the G2 + M phase cell population was the reverse to that on the SubG0/G1 phase, that is increasing after 48 h and decreasing again after 72 h. The number of MCF-7 cells that were in the G0/G1 and S phases after treatment with all concentrations of rHuEPO were essentially similar to that of the untreated group of control cells. It appeared that rHuEPO time-dependently affected the switching of MCF-7 cell population between the SubG0/G1 and G2 + M phases of the cell cycle. rHuEPO, especially at high concentrations, induced MCF-7 cells to enter the SubG0/G1 phase. Treatment with 0.1 to 100 IU/mL rHuEPO after 48 h caused the MCF-7 cells to transiently enter the G2 + M phase before shifting into the SubG0/G1 phase again after 72 h of treatment. 200 IU/mL

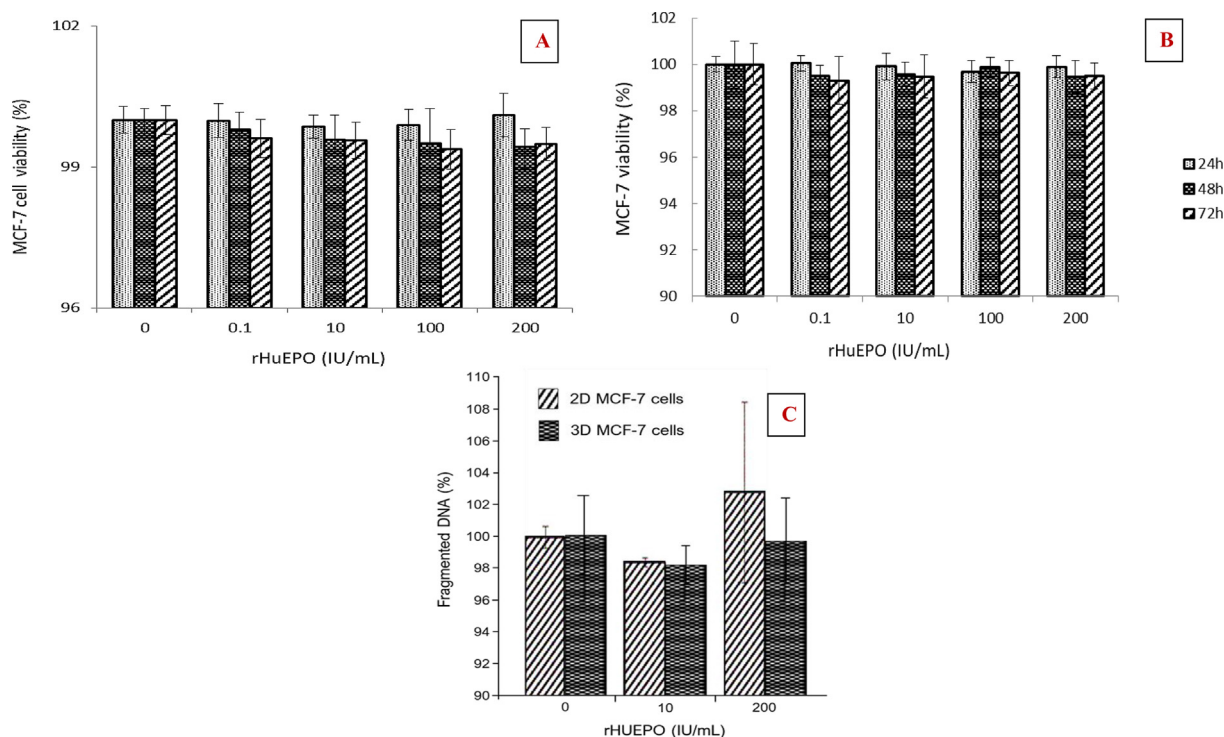


**Fig. 2.** (A) Effect of rHuEPO on viability of MCF-7 cells from 2D cultures determined by trypan blue exclusion assay. MCF-7 cell viability not significantly ( $p > 0.05$ ) affected by rHuEPO treatment. (B) Effect of rHuEPO on viability of MCF-7 cells from the 3D cell cultures determined by trypan blue exclusion assay. MCF-7 cell viability not significantly ( $p > 0.05$ ) affected by rHuEPO treatment. (C) Effect of rHuEPO on apoptosis of MCF-7 cells from 2D and 3D cultures determined by quantification of DNA fragmentation. There is no significant difference in the effect of rHuEPO on 2D and 3D cells and among treatment concentrations ( $p > 0.05$ ). Values are expressed as % of control. \*For each treatment period, means significantly different ( $p < 0.05$ ) from control means. Error bars represent RSE.

rHuEPO treatment had the greatest effect on the MCF-7 population, affecting the SubG0/G1 phase with 620% more treated than untreated control MCF-7 cells entering this phase of the cell cycle after 24 h. The number decreased again to 240% of the control after 72 h of rHuEPO treatment.

#### Caspases

Treatment with rHuEPO resulted in significant decreases in caspase-3, -8, and -9 activities of the 3D culture MCF-7 cells (Fig. 6). This effect became more prominent ( $p < 0.05$ ) with increase in rHuEPO concentration.

#### 4. Discussion

The 2D cell cultures, in spite of not approximating the *in vivo* form of tumors are still the *in vitro* models of choice in cancer studies. This is primarily due to the fact these models are stable and relatively easy to develop and use. *In situ* tumors are not 2D or monolayered, instead they are complex 3-dimensional structures with depths and components that are not easily accessible by therapeutic compounds. The 3D cell culture systems serve as relevant intermediates between the *in vitro* and *in vivo* cancer models, thus, they are more appropriate platforms than the 2D systems for the evaluation of anti-cancer compounds (Mikhail et al., 2013).

In this study, it was shown that rHuEPO affected proliferation of MCF-7 cells from the 3D not the 2D cultures. The effect of rHuEPO on MCF-7 cells in cultures is primarily dependent on chance interaction between rHuEPO and the EPORs. Since the binding of EPO to EPOR is not covalent in nature (Harris et al., 1992), the rHuEPO-EPOR interactions in cultures are expected to be reversible, depending on equilibrium of reaction and concentration of rHuEPO in the incubation medium. As spheroids, the MCF-7 cells from 3D cultures have mass and depth and some amount of scaffold and

matrix that allow for the cells to form tight aggregates. Therapeutic compounds like rHuEPO do not only interact with exposed cells on the surface of the 3D MCF-7 cell mass but may also perfuse into the matrix to affect the core and produce longer and more sustained effects (Millard et al., 2017).

rHuEPO time- and dose-dependently reduced viability of MCF-7 cells from 3D but not 2D cultures. rHuEPO also significantly and dose-dependently reduced the caspase-3, -8, and -9 activities of MCF-7 cells from the 3D culture. From these observations, it seemed that rHuEPO either slowed or inhibited proliferation of 3D culture MCF-7 cells; effects that are not associated with induction of cell death (Koçak et al., 2013). This is obvious because most apoptotic assays used in the study showed that rHuEPO did not significantly induce apoptosis of the MCF-7 cells. These findings suggest that rHuEPO had cytostatic rather than cytotoxic or apoptotic effect on MCF-7 cells from the 3D culture.

While some studies suggested EPO inhibits, others suggested it activates caspase activities in cancer cells (Chong et al., 2003; Wang et al., 2009; Liu et al., 2010). Whatever the effect of EPO on caspases, it is obvious that the results suggest that the anti-cancer effect of rHuEPO was not caspase-dependent, in fact, it can be mediated through mechanisms other than induction of cell death (Lee et al., 2012). However, the antiproliferative effects of anticancer compounds are not primarily through induction of cell death; it could be through a number of other mechanisms, including autophagy and cell cycle arrest (Semperebon et al., 2015; Mitra et al., 2018; D'Arcy, 2019). Since apoptosis, especially, the intrinsic pathway, requires the activation of caspases (McIlwain et al., 2013), it appears the cell death was not the mechanism of antiproliferative effect of rHuEPO on MCF-7 cells from 3D culture. In our study, rHuEPO increased population of MCF-7 entering the quiescent SubG0/G1 phase of the cell cycle. This phenomenon, along with the down-regulation of caspases, would suggest that the

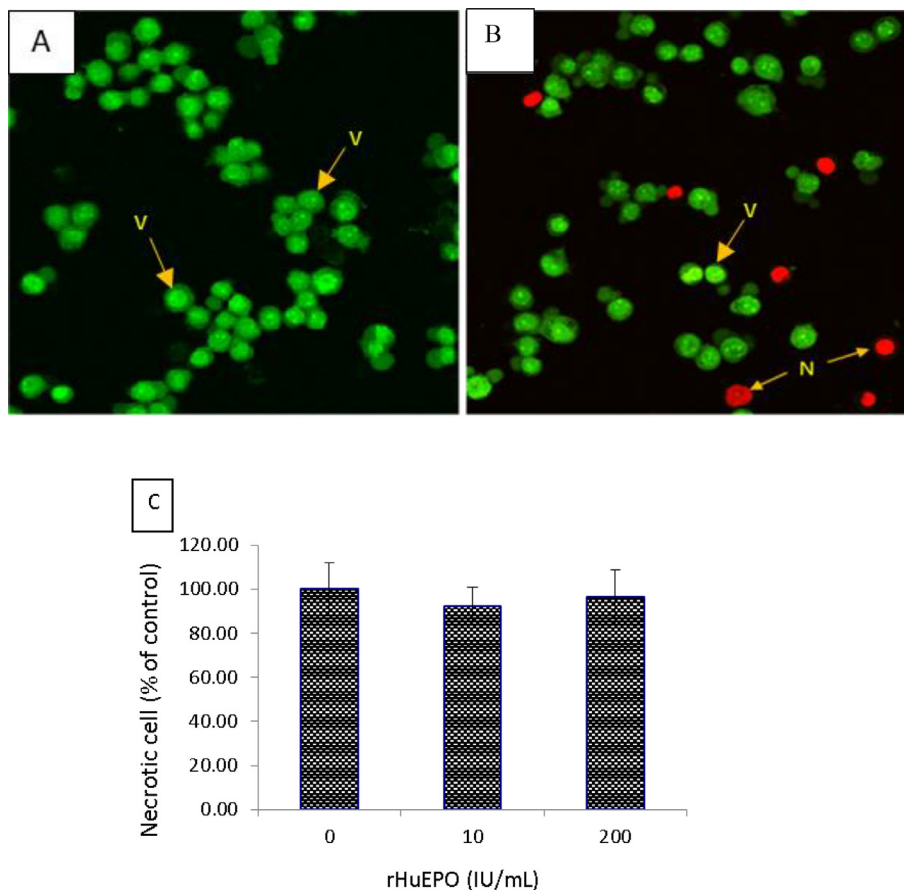


**Fig. 3.** Effect of rHuEPO on the morphology of MCF-7 cells from the 2D and 3D cultures determined by acridine orange/propidium iodide double-staining. rHuEPO treatments did not cause significant ( $p > 0.05$ ) change in morphology in 2D and 3D culture compared to untreated control cells. (A) representative image of treated and untreated 2D culture MCF-7 cells. (B) representative image of treated and untreated 3D culture MCF-7 cells. Although, treated 3D MCF-7 cells appeared to show some necrotic cells, there was no significant difference ( $p > 0.05$ ) in their numbers between treated and untreated cells. (C) Rate of MCF-7 cell necrosis in treated and untreated of 3D MCF-7 cell cultures. There was no significant difference ( $p > 0.05$ ) in necrotic cell number in treated and untreated cells group. The necrotic cells are those from the core of the spheroids. V: viable cells, N: necrotic cells. Values are expressed as % of control. Error bars represent RSE.

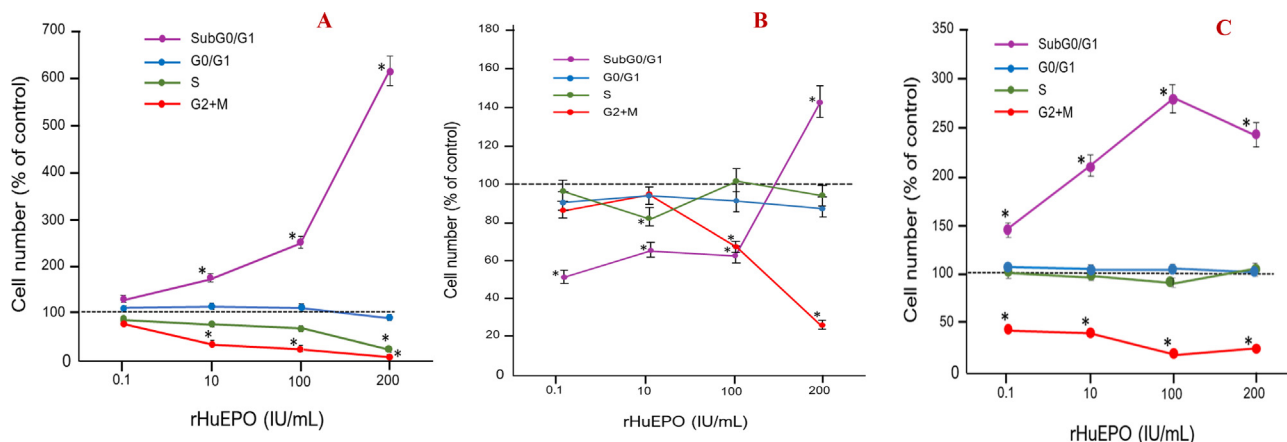


**Fig. 4.** (A) Effect of rHuEPO on 3D culture MCF-7 cell cycle after 24 h. rHuEPO primarily caused marked increase ( $p < 0.05$ ) in MCF-7 cells in the SubG0/G1 phase and mildly decreased ( $p < 0.05$ ) in those in the G2 + M phase. No significant change in the cells entering the G0/G1 phase ( $p > 0.05$ ) while in the S phase, cells decreased with treatment. (B) Effect of rHuEPO on 3D culture MCF-7 cell cycle after 48 h. rHuEPO only at 200 IU/mL primarily caused marked increase ( $p < 0.05$ ) MCF-7 in the SubG0/G1 phase and decrease ( $p < 0.05$ ) in the G2 + M phase. The cells in the G0/G1 and S although appeared to change with treatment, were variably close to the untreated control in number. (C) Effect of rHuEPO on 3D culture MCF-7 cell cycle after 72 h. At this treatment period, rHuEPO at all concentrations marked increased ( $p < 0.05$ ) MCF-7 cell population in the SubG0/G1 phase and decreased cells in the G2 + M phase. Values are expressed as % of control. \*For each treatment concentration, means significantly different ( $p < 0.05$ ) from control means. Broken line represents control value. Error bars represent RSE.

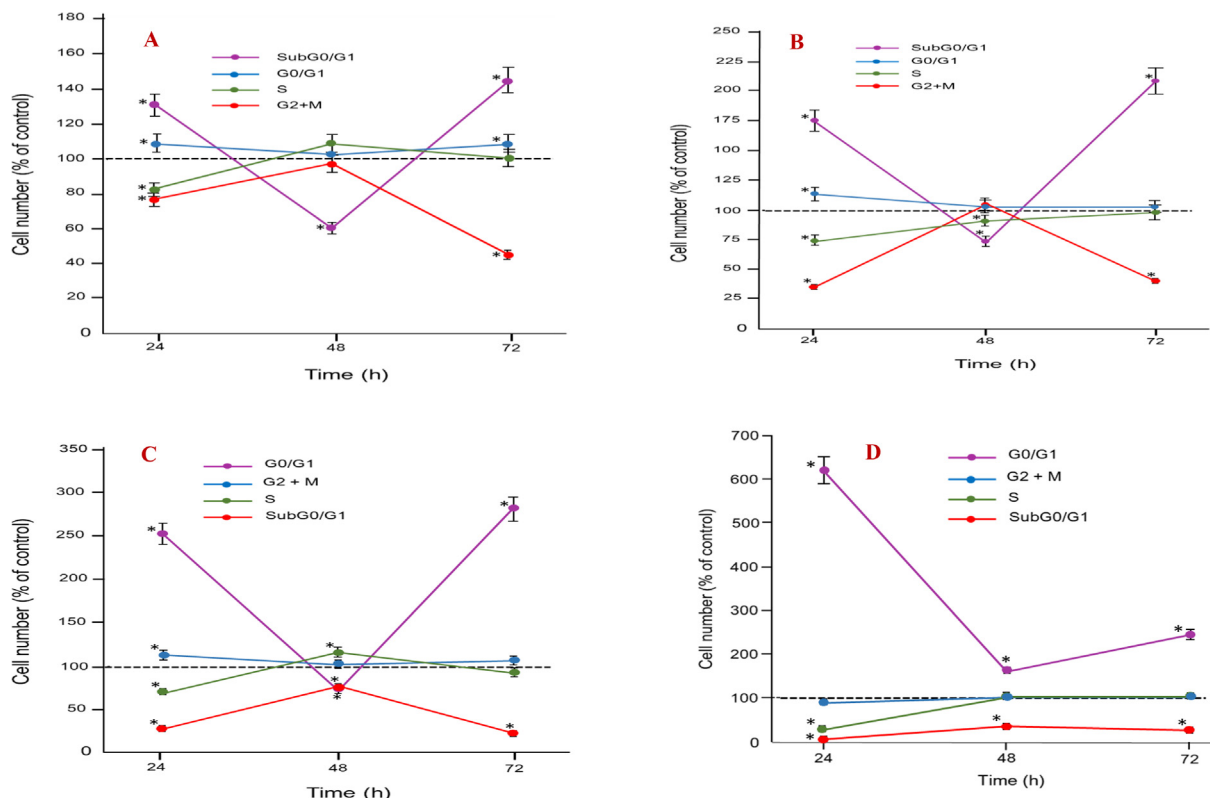


**Fig. 5.** Effect of (A) (0.1 IU/mL), (B) (10 IU/mL), (C) (100 IU/mL) and (D) (200 IU/mL) rHuEPO on 3D culture MCF-7 cell cycle. The subG0/G1 MCF-7 cell population was lowest and the G2 + M cells highest in number after 48 h of treatment. Values are expressed as % of control. \*For each treatment concentration, means significantly different ( $p < 0.05$ ) from control means. Error bars represent RSE. Broken line represents control value.

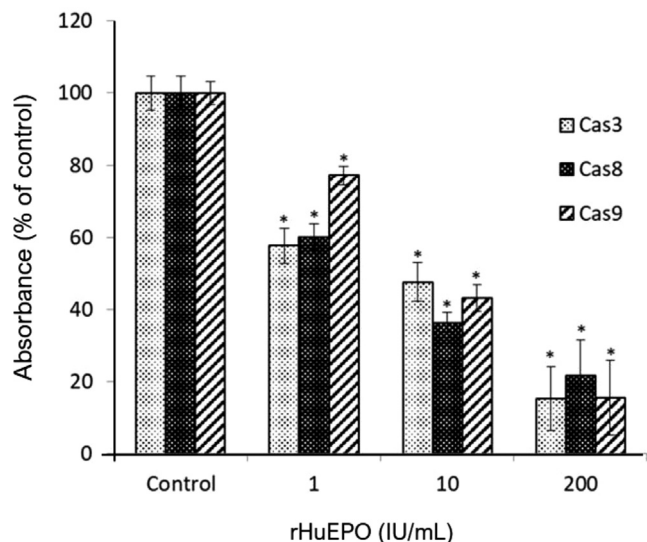


**Fig. 6.** Caspase activities of 3D culture MCF-7 cells treated with rHuEPO for 72 h. rHuEPO treatment significantly ( $p < 0.05$ ) cause decreased in caspases activities in a dose-dependent manner. The activities of caspase-3, -8 and -9 decreased with increase in treatment concentration. \*For treatment concentrations, means significantly different ( $p < 0.05$ ) from control means. Values are expressed as % of control. Error bars represent RSE. Cas3 = caspase-3, Cas8 = caspase-8, Cas9 = caspase-9.

rHuEPO induced the MCF-7 cells to enter a state of survival (Xu et al., 2018). It is possible that the action rHuEPO on cancer cells is similar to that on the erythroid progenitors in the bone marrow (Jelkmann, 2011), where cells under the effect of endogenous EPO are primed for survival and production of erythrocytes.

One study reported that EPO inhibited the proliferation of T-cells without inducing cell death (Cravedi et al., 2014), a mechanism proposed to be in effect in the rHuEPO-treated MCF-7 cell from 3D culture. Previous studies showed that the effect of EPO on cancer cells are conflicting. This is primarily due to the variability in conditions employed, which included cancer cell types and culture microenvironment such as the oxygen tension. Unlike the monolayer cells in 2D cultures, the MCF-7 cell spheroids from 3D cultures have hypoxic cores. Naturally, the effect of EPO on MCF-7 cells of the 2D will be different from that of the 3D cultures. Under hypoxic conditions, the hypoxia-inducible factor (HIF1- $\alpha$ ) is activated, leading to over-expression of vascular endothelial growth factor (Shi and Fang, 2004). HIF1- $\alpha$  and VEGF expressions are associated with aggressive cancer phenotype (Sa-Nguanraksa et al., 2015; Nalwoga et al., 2016). High expression of HIF1- $\alpha$  reflects metastatic potential, loss of apoptotic activity and poor patient overall survival in breast cancers (Bos et al., 2003; Semenza, 2009; Zhang et al., 2017). Furthermore, it was suggested that VEGF production by breast cancer cells promotes cell growth by an autocrine mechanism (Guo et al., 2003). Thus, targeting HIF1- $\alpha$  by inhibitory therapeutic agents will reduce aggressiveness and metastatic and angiogenic activities of breast cancers. Previous studies showed that under hypoxic condition, EPO inhibited HIF1- $\alpha$  activities in the ovarian cancer cells (Hale et al., 2006). The downregulation of VEGF due to HIF1- $\alpha$  inhibition was reported to reduce cancer cell growth (Wei et al. 2013). Thus, by virtue of the hypoxic core, rHuEPO is expected to be more effective at inhibiting proliferation of MCF-7 cells from 3D than the 2D cultures. This effect was evident in our study.

The 2D cell cultures used in cancer research have limitations such as inappropriate cell-cell and cell-extracellular environment interactions, expression of cell morphology, polarity, and cell

division while not representing solid tumors (Kapałczyńska et al., 2018). With the use of 3D cell cultures, the gap between *in vitro* cell cultures and *in vivo* tumors is partially bridged (Hoarau-Véchet et al., 2018). Cell spheroids provide better cell–cell and cell–matrix interactions than monolayer cells. These features are important in the determination of tumor cell cycle responses to therapeutic interventions, because cell cycle progression is regulated by cell-to-cell interactions through the integrins, the adhesion cell surface receptors determining cell proliferation (Moreno-Layseca and Streuli, 2014). In fact, cells under high intercellular tension exhibits greater transition from G1 to S and shorter G1 and S-G1-M phases (Uroz et al., 2018). We reported that rHuEPO caused the population of MCF-7 cells to enter the SubG0/G1 phase. This was evident by the marked increase in this cell cycle phase with concomitant decrease of cells in the G2 + M phase. These effects were most significant with high dose rHuEPO treatments.

Our study showed that rHuEPO down-regulated the caspase activities in the MCF-7 cells from 3D cultures. rHuEPO under certain conditions can block mitochondrial membrane depolarization and the release of cytochrome c (Hou et al., 2011; Shang et al., 2011), inhibiting downstream activation of the caspases and apoptosis. In mammary gland cancer cells EPOR are not only located on the cell membrane but also intracellularly, surrounding the nucleus (Arcasoy et al., 2002; Beh et al., 2019). This suggests that rHuEPO can bypass the surface receptor-mediated action and directly exert effects on the nucleus and without affecting caspase activities. This phenomenon seems to fit into the scheme of our study where rHuEPO is anti-proliferative towards 3D culture MCF-7 cells and by evidences from cell cycle analysis, may have induced cytostatic effect via caspase-independent cell death (CICD) (Dhuriya and Sharma, 2018; Roumane et al., 2018; Gong et al., 2019) instead of caspase-dependent apoptosis. The cell cycle study shows that rHuEPO is antiproliferative towards the MCF-7 cells by inducing the cells to enter the quiescent phase, subG0/G1.

## 5. Conclusion

To the best of our knowledge, this is the first study that investigated the effect of rHuEPO on the viability of MCF-7 breast cancer cells grown in 3D cultures. Based on the evidences in this study, rHuEPO inhibits MCF-7 cancer cell proliferation in 3D cell cultures. The primary modulator of the anti-cancer effect of rHuEPO is hypoxia, a condition that is present in the cancer cell spheroids of the 3D and not in monolayer cells of the 2D cultures. The study highlighted the importance of using 3D cultures in determining the anti-cancer effects of rHuEPO.

## Funding

This work was supported by the Malaysian Ministry of Science, Technology and Innovation IRPA grant 03-02-04-0563-SR0008/05-04.

## Declaration of Competing Interest

The authors declared that there is no conflict of interest.

## References

Acs, G., Acs, P., Beckwith, S.M., Pitts, R.L., Clements, E., Wong, K., Verma, A., 2001. Erythropoietin and erythropoietin receptor expression in human cancer. *Cancer Res.* 61 (9), 3561–3565.

Arcasoy, M., Amin, K., Karayal, A.F., Chou, S.-C., Raleigh, J.A., Varia, M.A., Haroon, Z.A., 2002. Functional Significance of Erythropoietin Receptor Expression in Breast

Cancer. *Lab. Invest.* 82, 911–918. <https://doi.org/10.1097/01.LAB.0000020415.72863.40>.

Bank, H.L., 1988. Rapid assessment of islet viability with acridine orange and propidium iodide. *Vitro Cell. Dev. Biol.* 24, 266–273. <https://doi.org/10.1007/BF02628826>.

Beh, C.Y., Rasedee, A., Selvarajah, G.T., Yazan, L.S., Omar, A.R., Foong, J.N., How, C.W., Foo, J.B., 2019. Enhanced anti-mammary gland cancer activities of tamoxifen-loaded erythropoietin-coated drug delivery system. *PLoS ONE* 14, (7). <https://doi.org/10.1371/journal.pone.0219285> e0219285.

Bos, R., van der Groep, P., Greijer, A.E., Shvarts, A., Meijer, S., Pinedo, H.M., Semenza, G.L., van Diest, P.J., van der Wall, E., 2003. Levels of hypoxia-inducible factor-1 $\alpha$  independently predict prognosis in patients with lymph node negative breast carcinoma. *Cancer* 97 (6), 1573–1581.

Burton, K., 1956. A study of the conditions and mechanism of the diphenylamine reaction for the colorimetric estimation of deoxyribonucleic acid. *Biochem. J.* 62, 315–323.

Cao, Y., Lathia, J.D., Eyler, C.E., Wu, Q., Li, Z., Wang, H., McLendon, R.E., Hjelmeland, A. B., Rich, J.N., 2010. Erythropoietin receptor signaling through STAT3 is required for glioma stem cell maintenance. *Genes Cancer* 1 (1), 50–61. <https://doi.org/10.1177/1947601909356352>.

Chong, Z.Z., Kang, J.-Q., Maiese, K., 2003. Apaf-1, Bcl-xL, cytochrome c, and caspase-9 form the critical elements for cerebral vascular protection by erythropoietin. *J. Cereb. Blood Flow Metab.* 23, 320–330. <https://doi.org/10.1097/01.WCB.0000050061.57184.AE>.

Cravedi, P., Manrique, J., Hanlon, K.E., Reid-Adam, J., Brody, J., Prathuangasuk, P., Mehrotra, A., Heeger, P.S., 2014. Immunosuppressive effects of erythropoietin on human alloreactive T cells. *J. Am. Soc. Nephrol.* 25, 2003–2015. <https://doi.org/10.1681/ASN.2013090945>.

D'Arcy, M.S., 2019. Cell death: a review of the major forms of apoptosis, necrosis and autophagy. *Cell* 43 (6), 582–592. <https://doi.org/10.1002/cbin.11137>.

Debeljak, N., Peter Solár, P., Arthur J. Sytkowski, A. J., 2014. Erythropoietin and cancer: the unintended consequences of anemia correction. *Front. Immunol.* 5, Article 563. <https://doi.org/10.3389/fimmu.2014.00563>

Dhuriya, Y.K., Sharma, D., 2018. Necroptosis: a regulated inflammatory mode of cell death. *J. Neuroinflammation* 15 (Article 199). <https://doi.org/10.1186/s12974-018-1235-0>.

Frille, A., Leithner, K., Olschewski, A., Olschewski, H., Wohlkönig, C., Hrzenjak, A., 2018. No erythropoietin-induced growth is observed in non-small cell lung cancer cells. *Int. J. Oncol.* 52, 518–526. <https://doi.org/10.3892/ijo.2017.4225>.

Fujisue, Y., Nakagawa, T., Takahara, K., Inamoto, T., Kiyama, S., Azuma, H., Asahi, M., 2013. Induction of erythropoietin increases the cell proliferation rate in a hypoxia-inducible factor-1-dependent and -independent manner in renal cell carcinoma cell lines. *Oncol. Lett.* 5, 1765–1770. <https://doi.org/10.3892/ol.2013.1283>.

Gong, Y., Fan, Z., Luo, G., Yang, C., Huang, Q., Fan, K., Cheng, H., Jin, K., Ni, Q., Yu, X., Liu, C., 2019. The role of necroptosis in cancer biology and therapy. *Mol. Cancer*, 18, 100. <https://molecular-cancer.biomedcentral.com/articles/10.1186/s12943-019-1029-8>

Guo, P., Fang, Q., Tao, H.-Q., Schafer, C.A., Fenton, B.M., Ding, I., Hu, B., Cheng, S.-Y., 2003. Overexpression of vascular endothelial growth factor by MCF-7 breast cancer cells promotes estrogen-independent tumor growth *in vivo*. *Cancer Res.* 63, 4684–4691.

Hale, S.A., Wong, C., Lounsbury, K.M., 2006. Erythropoietin disrupts hypoxia-inducible factor signaling in ovarian cancer cells. *Gynecol. Oncol.* 100, 14–19.

Harris, K.W., Mitchell, R.A., Winkelman, J.C., 1992. Ligand binding properties of the human erythropoietin receptor extracellular domain expressed in *Escherichia coli*. *J. Biol. Chem.* 267, 15205–15209.

Hoarau-Véchet, J., Rafii, A., Touboul, C., Pasquier, J., 2018. Halfway between 2D and animal models: are 3D cultures the ideal tool to study cancer-microenvironment interactions? *Int. J. Mol. Sci.*, 19(1),181. <https://doi.org/10.3390/ijms19010181>.

Hou, J., Wang, S., Shang, Y.C., Chong, Z.Z., Maiese, K., 2011. Erythropoietin employs cell longevity pathways of SIRT1 to foster endothelial vascular integrity during oxidant stress. *Curr. Neurovasc. Res.* 8 (3), 220–235. <https://doi.org/10.2174/156720211796558069>.

Ilkovičová, L., Trošt, N., Szentpéteri, E., Solár, P., Komel, R., Debeljak, N., 2017. Overexpression of the erythropoietin receptor in RAMA37 breast cancer cells alters cell growth and sensitivity to tamoxifen. *Int. J. Oncol.* 51, 737–746. <https://doi.org/10.3892/ijo.2017.4061>.

Jelkmann, W., 2011. Regulation of erythropoietin production. *J. Physiol.* 589, 1251–1258. <https://doi.org/10.1113/jphysiol.2010.195057>.

Kapałczyńska, M., Kolenda, T., Przybyła, W., Zajáčzkowska, M., Teresiak, A., Filas, V., Ibb, M., Bliźniak, R., Łuczewski, Ł., Lamperska, K., 2018. 2D and 3D cell cultures – a comparison of different types of cancer cell cultures. *Arch. Med. Sci.* 14(4), 910–919. <https://doi.org/10.5114/aoms.2016.63743>.

Klemm, K., Eipel, C., Cantré, D., Abshagen, K., Menger, M.D., Vollmar, B., 2008. Multiple doses of erythropoietin impair liver regeneration by increasing TNF- $\alpha$ , the Bax to Bcl-xL ratio and apoptotic cell death. *PLOS ONE* 3. <https://doi.org/10.1371/journal.pone.0003924> e3924.

Koçak, F.E., Erdoğan, E., Ozyigit, F., Yerlikaya, A., 2013. Evaluation of antiproliferative and antimetastatic effects of heparin and erythropoietin on B16f10 melanoma cell line. *Cell. Mol. Biol. (Noisy -le-grand)*. Fr. 59 Suppl, OL1894–1898.

Kumar, P., Nagarajan, A., Uchil, P.D., 2018. Analysis of cell viability by the MTT assay. *Cold Spring Harb. Protoc.* 2018 (6). <https://doi.org/10.1101/pdb.prot095505>.

Lee, Y.J., Won, A.J., Lee, J., Jung, J.H., Yoon, S., Lee, B.M., Kim, H.S., 2012. Molecular mechanism of saha on regulation of autophagic cell death in tamoxifen-

- resistant MCF-7 breast cancer cells. *Int. J. Med. Sci.* 9, 881–893. <https://doi.org/10.7150/ijms.5011>.
- Liu, Y.-Y., She, Z.-J., Yao, M.-H., 2010. Erythropoietin inhibits  $\gamma$ -irradiation-induced apoptosis by upregulation of Bcl-2 and decreasing the activation of caspase 3 in human UT-7/erythropoietin cell line. *Clin. Exp. Pharmacol. Physiol.* 37, 624–629. <https://doi.org/10.1111/j.1440-1681.2010.05370.x>.
- Louis, K.S., Siegel, A.C., 2011. Cell Viability Analysis Using Trypan Blue: Manual and Automated Methods, in: Stoddart, M.J. (Ed.), *Mammalian Cell Viability, Methods in Molecular Biology*. Humana Press, pp. 7–12.
- McIlwain, D. R., Berger, T., Mak, T. W. (2013). Caspase functions in cell death and disease. *Cold Spring Harb Perspect Biol*, 5(4), a008656. <https://doi.org/10.1101/cshperspect.a008656>.
- Mikhail, A.S., Etezeadi, S., Allen, C., 2013. Multicellular tumor spheroids for evaluation of cytotoxicity and tumor growth inhibitory effects of nanomedicines in vitro: a comparison of docetaxel-loaded block copolymer micelles and Taxotere®. *PLoS ONE* 8. <https://doi.org/10.1371/journal.pone.0062630>. e62630.
- Millard, M., Yakavets, I., Zorin, V., Kulmukhamedova, A., Marchal, S., Bezdetnaya, L., 2017. Drug delivery to solid tumors: the predictive value of the multicellular tumor spheroid model for nanomedicine screening. *Int. J. Nanomedicine* 12, 7993–8007. <https://doi.org/10.2147/IJN.S146927>.
- Mitra, M., Ho, L.D., Collier, H.A., 2018. An in vitro model of cellular quiescence in primary human dermal fibroblasts. *Methods Mol. Biol.* 1686, 27–47. [https://doi.org/10.1007/978-1-4939-7371-2\\_2](https://doi.org/10.1007/978-1-4939-7371-2_2).
- Morais, C., Johnson, D.W., Vesey, D.A., Gobe, G. C. 2013. Functional significance of erythropoietin in renal cell carcinoma. *BMC Cancer* 13, (14) (2013). <https://doi.org/10.1186/1471-2407-13-14>.
- Moreno-Layseca, P., Streuli, C.H., 2014. Signalling pathways linking integrins with cell cycle progression. *Matrix Biol. J. Int. Soc. Matrix Biol.* 34, 144–153. <https://doi.org/10.1016/j.matbio.2013.10.011>.
- Mosmann, T., 1983. Rapid colorimetric assay for cellular growth and survival: Application to proliferation and cytotoxicity assays. *J. Immunol. Methods* 65, 55–63. [https://doi.org/10.1016/0022-1759\(83\)90303-4](https://doi.org/10.1016/0022-1759(83)90303-4).
- Nairz, M., Schroll, A., Moschen, A.R., Sonnweber, T., Theurl, M., Theurl, I., Taub, N., Jannig, C., Neutrauer, D., Huber, L.A., Tilg, H., Moser, P.L., Weiss, G., 2011. Erythropoietin contrastingly affects bacterial infection and experimental colitis by inhibiting nuclear factor- $\kappa$ B-inducible immune pathways. *Immunity* 34(1), 61–74. <https://doi.org/10.1016/j.immuni.2011.01.002>.
- Nalwoga, H., Ahmed, L., Arnes, J.B., Wabinga, H., Aklsen, L.A., 2016. Strong expression of hypoxia-inducible factor-1 $\alpha$  (HIF-1 $\alpha$ ) is associated with Axl expression and features of aggressive tumors in African breast cancer. *PLOS ONE* 11 (1), e0146823. <https://doi.org/10.1371/journal.pone.0146823>.
- Nangaku, M., 2013. Tissue protection by erythropoietin: new findings in a moving field. *Kidney Int.*, 84, 427–429. <https://www.kidney-international.org/action/showPdf?pii=S0085-2538%2815%2955986-3>
- Okazaki, T., Ebihara, S., Asada, M., Yamada, S., Niu, K., Arai, H., 2008. Erythropoietin promotes the growth of tumors lacking its receptor and decreases survival of tumor-bearing mice by enhancing angiogenesis. *Neoplasia* 10(9), 932–939.
- Osato, K., Sato, Y., Osato, A., Sato, M., Zhu, C., Leist, M., Kuhn, H.G., Blomgren, K., 2018. Carbamylated erythropoietin decreased proliferation and neurogenesis in the subventricular zone, but not the dentate gyrus, after irradiation to the developing rat brain. *Front. Neurol.* 9. <https://doi.org/10.3389/fneur.2018.00738>.
- Pozarowski, P., Darzynkiewicz, Z., 2004. Analysis of Cell Cycle by Flow Cytometry. In: Schönthal, A.H. (Ed.), *Checkpoint Controls and Cancer: Volume 2: Activation and Regulation Protocols, Methods in Molecular Biology*. Humana Press, Totowa, NJ, pp. 301–311. 10.1385/1-59259-811-0:301.
- Reinbothe, S., Larsson, A.-M., Vaapil, M., Wigerup, C., Sun, J., Jögi, A., Neumann, D., Rönstrand, L., Pahlman, S., 2014. EPO-independent functional EPO receptor in breast cancer enhances estrogen receptor activity and promotes cell proliferation. *Biochem. Biophys. Res. Commun.* 445, 163–169. <https://doi.org/10.1016/j.bbrc.2014.01.165>.
- Riffle, S., Hedge, R.S., 2017. Modeling tumor cell adaptations to hypoxia in multicellular tumor spheroids. *J. Exp. Clin. Cancer Res.* 36 (1), 102. <https://doi.org/10.1186/s13046-017-0570-9>.
- Roumane, A., Berthenet, K., El Fassi, C., Ichim, G., 2018. Caspase-independent cell death does not elicit a proliferative response in melanoma cancer cells. *BMC Cell Biol.* 19. <https://doi.org/10.1186/s12860-018-0164-1>.
- Semperebon, S. C., Marques, L. A., D'Epiro, G. F., de Camargo, E. A., da Silva, G. N., Niwa, A. M., Macedo Junior, F., Mantovani, M. S., 2015. Antiproliferative activity of goniothalamin enantiomers involves DNA damage, cell cycle arrest and apoptosis induction in MCF-7 and HB4a cells. *Toxicol In Vitro.* 30(1 Pt B), 250–263. doi: 10.1016/j.tiv.2015.10.012.
- Shang, C.Y., Zhong Z.Z., Wang, S., Maiese, K., 2011. Erythropoietin and Wnt1 govern pathways of mTOR, Apaf-1, and XIAP in Inflammatory Microglia [WWW Document]. <https://doi.org/info:doi/10.2174/156720211798120990>.
- Shi, Y. H., Fang, W. G. 2004. Hypoxia-inducible factor-1 in tumour angiogenesis. *World journal of gastroenterology*, 10(8), 1082–1087. <https://doi.org/10.3748/wjg.v10.i8.1082>.
- Sa-Nguanraksa, D., Chuangsuwanich, T., Pongpruttipan, T., O-Chaorenrat, P., 2015. High vascular endothelial growth factor gene expression predicts poor outcome in patients with non-luminal A breast cancer. *Molecular and clinical oncology* 3 (5), 1103–1108. <https://doi.org/10.3892/mco.2015.574>.
- Semenza, G.L., 2009. Regulation of cancer cell metabolism by hypoxia-inducible factor 1. *Semin Cancer Biol* 19, 12–16.
- Suenobu, N., Shichiri, M., Iwashina, M., Marumo, F., Hirata, Y., 1999. Natriuretic Peptides and Nitric Oxide Induce Endothelial Apoptosis via a cGMP-Dependent Mechanism. *Arterioscler. Thromb. Vasc. Biol.* 19 (1), 140–146. <https://doi.org/10.1161/01.ATV.19.1.140>.
- Tankiewicz-Kwedlo, A., Hermanowicz, J., Surazynski, A., Rożkiewicz, D., Pryczynicz, A., Domaniewski, T., Pawlak, K., Kemona, A., Pawlak, D., 2016. Erythropoietin accelerates tumor growth through increase of erythropoietin receptor (EpoR) as well as by the stimulation of angiogenesis in DLD-1 and Ht-29 xenografts. *Mol. Cell. Biochem.* 421, 1–18. <https://doi.org/10.1007/s11010-016-2779-x>.
- Teo, G.Y., Rasedee, A., Al-Haj, N.A., Beh, C.Y., How, C.W., Rahman, H.S., Alitheen, N.B., Rosli, R., Abdullah, A.H., Ali, A.S., 2020. Effect of fetal bovine serum on erythropoietin receptor expression and viability of breast cancer cells. *Saudi Journal of Biological Sciences.* 27 (2), 653–658. <https://doi.org/10.1016/j.sjbs.2019.11.032>.
- Todaro, M., Turdo, A., Bartucci, M., Iovino, F., Dattilo, R., Biffoni, M., Stassi, G., Federici, G., De Maria, R., Zeuner, A., 2013. Erythropoietin activates cell survival pathways in breast cancer stem-like cells to protect them from chemotherapy. *Cancer Res.* 73, 6393–6400. <https://doi.org/10.1158/0008-5472.CAN-13-0248>.
- Uroz, M., Wistorf, S., Serra-Picamal, X., Conte, V., Sales-Pardo, M., Roca-Cusachs, P., Guimerà, R., Trepac, X., 2018. Regulation of cell cycle progression by cell-cell and cell-matrix forces. *Nat. Cell Biol.* 20, 646–654. <https://doi.org/10.1038/s41556-018-0107-2>.
- Wang, Y., Zhao, L., Lu, F., Yang, X., Deng, Q., Ji, B., Huang, F., 2015. Retinoprotective effects of bilberry anthocyanins via antioxidant, anti-inflammatory, and anti-apoptotic mechanisms in a visible light-induced retinal degeneration model in pigmented rabbits. *Mol. Basel Switz.* 20, 22395–22410. <https://doi.org/10.3390/molecules201219785>.
- Wang, Z., Xiong, J., Yang, X., Li, Y., Xu, Z., Cui, L., Wang, F., Tan, L., Zhang, L., 2009. Effect of erythropoietin on the caspase-3 subfamily in preventing apoptosis of endothelial cell. *Zhongguo Wei Zhong Bing Ji Jiu Yi Xue Chin. Crit. Care Med. Zhongguo Weizhongbing Jijiu yixue* 21(12), 711–714.
- Wei, D., Peng, J.-J., Gao, H., Li, H., Li, D., Tan, Y., Zhang, T., 2013. Digoxin downregulates NDRG1 and VEGF through the inhibition of HIF-1 $\alpha$  under hypoxic conditions in human lung adenocarcinoma A549 cells. *Int. J. Mol. Sci.* 14, 7273–7285. <https://doi.org/10.3390/ijms14047273>.
- Xu, D.C., Arthurton, L., Baena-Lopez, L.A., 2018. Learning to fly: the interplay between caspases and cancer. *Biomed. Res. Int.*, 2018, Article ID 5473180 <https://doi.org/10.1155/2018/5473180>
- Zhang, Y., Yan, J., Wang, L., Dai, H., Li, N., Hu, W., Cai, H., 2017. HIF-1 $\alpha$  promotes breast cancer cell MCF-7 proliferation and invasion through regulating miR-210. *Cancer Biother. Radiopharm.* 32(8), 297–301. <https://doi.org/10.1089/cbr.2017.2270>.